Prolonged stimulation of a brainstem raphe region attenuates experimental autoimmune encephalomyelitis

Madsen, Pernille Marie; Sloley, Stephanie S.; Vitores, Alberto A.; Carballosa-Gautam, Melissa M.; Brambilla, Roberta; Hentall, Ian D.

Published in:
Neuroscience

DOI:
10.1016/j.neuroscience.2017.01.037

Publication date:
2017

Document version
Peer reviewed version

HHS Public Access

Author manuscript

Neuroscience. Author manuscript; available in PMC 2018 March 27.

Published in final edited form as:

Neuroscience. 2017 March 27; 346: 395–402. doi:10.1016/j.neuroscience.2017.01.037.

Prolonged Stimulation of a Brainstem Raphe Region Attenuates Experimental Autoimmune Encephalomyelitis

Pernille M. Madsen[a], **Stephanie S. Sloley**[a], **Alberto A. Vitores**[a], **Melissa M. Carballosa-Gautam**[a], **Roberta Brambilla**[a], and **Ian D. Hentall**[a]

[a]The Miami Project to Cure Paralysis, University of Miami Miller School of Medicine, Miami, USA

[b]Department of Neurobiology Research, Institute of Molecular Medicine, University of Southern Denmark, Odense, Denmark

Abstract

Multiple sclerosis (MS), a neuroinflammatory disease, has few treatment options, none entirely adequate. We studied whether prolonged electrical stimulation of a hindbrain region (the nucleus raphe magnus) can attenuate experimental autoimmune encephalomyelitis, a murine model of MS induced by MOG35-55 injection. Eight days after symptoms emerged, a wireless electrical stimulator with a connectorless protruding microelectrode was implanted cranially, and daily intermittent stimulation of awake, unrestrained mice began immediately. The thoracic spinal cord was analyzed for changes in histology (on day 29) and gene expression (on day 37), with a focus on myelination and cytokine production. Controls, with inactive implants, showed a phase of disease exacerbation on days 19–25 that stimulation for >16 days eliminated. Prolonged stimulation also reduced infiltrating immune cells and increased numbers of myelinated axons. It additionally lowered gene expression for some pro-inflammatory cytokines (interferon gamma and tumor necrosis factor) and for platelet-derived growth factor receptor alpha, a marker of oligodendrocyte precursors, while raising it for myelin basic protein. Restorative treatments for MS might profitably consider ways to stimulate the raphe magnus, directly or via its inputs, or to emulate its serotonergic and peptidergic output.

Keywords

nucleus raphe magnus; multiple sclerosis; deep brain stimulation; cytokines; myelination

Introduction

Multiple sclerosis (MS) is a chronic autoimmune disease characterized by localized destruction of the myelin sheets that enwrap and support axons of the central nervous system (CNS) (Friese et al., 2014; Mohan et al., 2014). The etiology is unknown and a satisfactory

Corresponding Author Until Publication: i.hentall@miami.edu. Corresponding Author After Publication: r.brambilla@miami.edu.

cure is elusive. Current therapies are limited to systemic administration of immune-modulating agents that can reduce infiltration of peripheral immune cells and thereby dampen inflammatory signals in the CNS (Minagar, 2013; Ransohoff et al., 2015). An alternative possible approach, as in the present paper, is to address directly the loss of myelin and axons that underlies the permanent disability of progressive forms of MS (Fitzner and Simons, 2010).

We previously showed that prolonged electrical stimulation in one of the serotonergic raphe nuclei of the brainstem promotes recovery after neurotrauma in rats. The ascending systems of the median or dorsal raphe of the midbrain, when stimulated intermittently for one week (8 Hz, 5 minutes on-off cycling, 12 hours daily) beginning several hours after traumatic brain injury, enhanced both behavioral and gross anatomical recovery (Carballosa Gonzalez et al., 2013). The hindbrain's nucleus raphe magnus (NRM), a major source of spinal cord serotonin, similarly improved motor recovery from spinal cord injury (Hentall and Burns, 2009; Hentall and Gonzalez, 2012) while augmenting myelin sparing and serotonergic innervation around the injury site. Consistent with a primarily restorative role, all tested raphe regions proved to be non-eloquent, evoking no apparent motor or aversive effects and thus allowing problem-free prolonged stimulation.

These prior results suggested that raphe stimulation could reduce or even reverse the functional and anatomical degeneration associated with progressive forms of MS. A first exploration of this possibility is reported here. We studied a common mouse model of MS, experimental autoimmune encephalomyelitis (EAE), which is induced by injection of myelin-derived peptides (Procaccini et al., 2015) and tends to cause strong spinal cord deficits. The NRM was selected as the stimulation target because of its direct descending projection and its previously demonstrated benefits for myelination. The analysis included a daily score of overt symptoms (EAE score), histological examination of myelination and tissue infiltration, and real-time polymerase chain reaction (PCR) measurement of expression for myelination-related proteins and cytokines in thoracic spinal cord. Injection of the 35-55 peptide fragment of myelin oligodendrocyte glycoprotein (MOG_{35-55}) caused a typical progression of overt disease in untreated animals: an acute inflammatory phase that reached a peak 4 to 6 days after the first symptoms emerged and a later exacerbation in approximately the 3rd week. Beyond this time point, untreated EAE declined rapidly, precluding study of more prolonged treatment; hence euthanasia was done on the 29th or 37th day. To minimize the surgical risks of general anesthesia during the acute phase and to obtain a stable baseline period of disease, the wireless electronic stimulator and integral electrode were implanted on the 8th day of symptoms. Long-term stimulation began immediately after implantation.

Materials and Methods

Study Design

Mice (20 control, 20 stimulated) were studied in four sequential batches, within which they were alternatingly assigned to stimulated and control groups. These group sizes were used because they equaled or exceeded group sizes giving satisfactory statistical power in prior studies of NRM stimulation for spinal cord injury and drug treatment for EAE (Hentall and

Gonzalez, 2012; Madsen et al., 2016). Clinical signs of EAE were assessed daily by the same trained and blinded observer. Later histological analysis was also conducted by persons blinded to the treatment. Days are numbered in this article with reference to EAE onset ("disease day") unless otherwise specified. Onset of symptoms occurred 20 ±0.9 days (mean ± SEM) after induction. Stimulators were implanted and the stimulation program activated on disease day 8. A control group was treated identically, except the implant remained inactive. The first two batches underwent euthanasia on disease day 29. The last two batches underwent euthanasia on disease day 37 ±1. Mice used in Subsets were selected for histological analysis at disease day 29 and for real-time PCR analysis at disease day 37 based on longevity of stimulation (≥17 days) and on the closest matching EAE scores on day 8 in controls.

The statistical analysis of EAE scores used SPSS (version 21: IBM Corp.). A two-sided significance level of $p \leq 0.05$ was applied; effect size (partial eta-squared) for individual variables is also reported when available. To examine the effect of stimulation on EAE scores, a repeated-measures analysis of variance (ANOVA) compared treated and control groups during disease exacerbation. Parametric t-tests for treatment differences on individual days were derived from the repeated measures software routine. To assess the mean time-course of EAE after cessation of stimulation, the score for a given day in each stimulated mouse was first subtracted from the mean control (untreated) EAE score for the same disease day, and days were then renumbered relative to their last day of stimulation, before being finally averaged across subjects for each post-stimulation day. The significance of the difference between a given day and all preceding days was provided by within-subject contrasts after repeated measures ANOVA. Results of real-time PCR were analyzed by the independent samples exact Mann-Whitney test and results of the histological quantification by unpaired (unequal variance) t-tests, both using Prism software (GraphPad Inc., version 6.05).

Mice

Six-week old female C57BL/6 mice were obtained from Jackson Laboratory. They were housed in individually ventilated cages in a virus/antigen-free facility on a 12-hour light/dark cycle and given free access to food and water. All experiments were performed in accordance with protocols and guidelines approved by the local Institutional Animal Care and Use Committee.

MOG_{35-55}-induced Experimental Autoimmune Encephalomyelitis

Active EAE was induced in mice aged 2–3 months by injection of MOG_{35-55} peptide, as described previously (Madsen et al., 2016). It was measured on a standard scale from 0 to 6, as follows: 0, no clinical signs; 1, loss of tail tone; 2, fully flaccid tail; 3, complete hind limb paralysis; 4, complete forelimb paralysis; 5, moribund; 6, dead (0.5 gradations were used for intermediate scores).

Stimulators

The self-powered, wireless, epoxy-embedded stimulators with infrared readout (Figs. 1A, B) were fabricated in-house based on a previously published design for rats (Hentall, 2013).

The main modifications were smaller size (dimensions 10 mm long, 5.5 mm wide and 5 mm high) and control by visible light instead of magnetic pulses. A commercially obtained tungsten microelectrode of 0.5 megohm nominal impedance (A-M Systems, Inc., Sequim, WA; catalog number 573210) emerged directly from the epoxy capsule along with a stainless steel wire anode. Through a step-up voltage regulator with current feedback, the microprocessor-based program delivered constant-current cathodal pulses of 30 μA amplitude and 1 ms duration at 8 Hz during 12 daylight hours in an alternating pattern of 5 minutes on and 5 minutes off. Pulses of amplitude 30 μA are estimated to activate the average NRM cell body within a radius of 190 μm, well inside the dimensions of the nucleus, based on measured threshold-distance relations in the rat's NRM (Hentall et al., 1984).

Surgical Implantation and Stimulation

Mice were anesthetized with 1.2% isoflurane in oxygen. The microelectrode was placed stereotaxically through a burr hole in the midline NRM (1.8 mm posterior and 5.8 mm below the interaural line in flat-skull orientation). The anode wire was wrapped around a stainless steel miniature screw in the skull. There was approximately 1 mm clearance between the stimulator capsule and skull. Dental cement fixed the stimulator to the screw and skull. The skin incision was closed posteriorly by sterile sutures. Post-operative care included subcutaneously injecting buprenorphine (0.2mg/kg bid for 3 days) for analgesia and gentamycin (5mg/kg bid for 7 days) to prevent infection. The status of the stimulation program was signaled by width-modulated infrared pulses, and was checked at least once per day by means of a custom-built reader. Failure to detect an infrared signal was taken to indicate a non-functional stimulator, and this status was ensured by applying the inactivating sequence of light pulses.

Perfusion and Histological Analysis

Mice used for histological analysis were euthanatized by i.p. injection of 100mg/kg ketamine and 10mg/kg xylazine. The brain and spinal cord were sectioned coronally at 1 μm thickness and stained with 1 % toluidine blue. Sections were examined by light microscopy (Zeiss) at 63X magnification and infiltrating cells, myelinated and collapsed axons were quantified by Stereoinvestigator (MicroBrightField Inc.) software. The number of infiltrating cells was expressed per area of section. Because the tissue area shrinks considerably with demyelination or axon collapse in EAE, axons were quantified simply by total count. Locations of stimulation electrodes were verified in a subset of mice by examining sagittal or coronal sections near the midline (n=8). Some brains were sectioned at 10 μm thickness and stained with hematoxylin-eosin. Other brains were cut as 30 μm sagittal sections immunostained with mouse anti-NeuN (1:500, Millipore), rabbit anti-GFAP (1:1000, Millipore) and Vectashield DAPI mounting medium (VectorLabs). Tips of the electrode proved always to lie in the cytologically defined region of the NRM (Figs. 1C, D). The electrode track was associated with mild astrocytic activity along the track and minimal tissue damage (Fig. 1C).

Total RNA isolation and Real-time PCR

Total RNA was isolated from PBS perfused, fresh frozen spinal cord tissue using Trizol Reagent (Invitrogen) in accordance with the manufacturer's protocol. Remaining DNA and protein residue was removed using the RNeasy Mini Kit (Qiagen) in combination with on-column DNA digestion using the RNase-Free DNase Set (Qiagen), performed in accordance with the manufacturer's protocol. For each sample, 0.5 mg RNA was reverse-transcribed with Omniscript RT kit (Qiagen). The complimentary DNA was used as template for a real time PCR reaction using the Rotor-Gene SYBR Green PCR Kit (Qiagen). Gene expression was quantified for myelin basic protein (MBP), Notch1, platelet-derived growth factor receptor alpha (PDGFRα), interferon gamma (IFNγ), interleukin-1β (IL-1β) and tumor necrosis factor (TNF), all normalized to expression of glyceraldehyde 3-phosphate dehydrogenase (GADPH). See Table 1 for gene-specific primer list.

Results

Effect of NRM stimulation on EAE scores

The planned timeline was to give stimulation until the day of euthanasia (Fig. 2A), but this was precluded by the stimulator battery lifetime, whose median was 17.5 days (estimated by Kaplan-Meir analysis, ± 1.8 SEM, n=20). Thus it was possible to give prolonged stimulation in most mice for the majority of days planned. Stimulated mice were divided into two main groups. One group (n=9) received longer stimulation that lasted through all or most of the late phase of disease exacerbation, occurring on disease days 19–26; the range of stimulator lifetimes was 17–29 days (until disease days 25–37). The late phase, readily apparent in controls (n=12), was essentially absent after the longer stimulation (Fig. 2B). The difference between the control group and the longer-stimulated group over the 7 days of disease exacerbation was statistically significant. Individual days within this 7-day range, except disease day 20, also showed significant treatment differences. Due to a rapid decline in untreated disease, EAE scores converged in control and stimulated groups around disease day 29. The other main group of stimulated mice (n=7) received 4–15 days of stimulation (until disease days 12–23). This shorter stimulation had no significant effect on the course of the mean EAE score referenced to the first day of symptoms (Fig. 2C).

The duration of effects beyond the end of stimulation was analyzed by averaging scores referenced to the last day of stimulation. Two ranges of stimulation were available, 4–7 days (n=4) and 15–21 days (n=6); beyond 21 days, the time series were too short to analyze. Stimulation for 4–7 days was followed by a growing difference between the falling score of this group and the more stable control score (Fig. 2D). The difference was visually apparent after 4 days and continued for 7 more days before subsiding over the next 4 days; it was significant on days 10 and 11 compared to prior days. In mice that received 15–21 days of stimulation, there was an immediate post-stimulation difference from the control scores that slowly disappeared over 6 days (Fig. 2D); the difference was significant on days 4 and 5.

Myelin, axon pathology and immune cell infiltration

A random sample of mice that received longer stimulation (mean 19.4 days ±1.5 SEM, n=5) were examined for histopathological damage on disease day 29 in comparison with a sample

of matched controls (n=5). Our previous studies have shown that the presence of EAE more than doubles immune cell infiltration and collapsed axons compared to non-diseased mice while numbers of myelinated fibers are less than half (Brambilla et al., 2011). All mice showed widespread axonal loss and immune cell infiltration that was visibly less severe in stimulated mice (Fig. 3A). Stimulation significantly increased the number of myelinated axons (Fig. 3B) and lowered the density of infiltrating cells in the white matter parenchyma (Fig. 3D). There was no significant difference detected in the number of collapsed (degenerating) axons (Fig. 3C).

Expression of myelin-related genes and pro-inflammatory cytokines

A different sample of longer-term stimulated mice (≥17 days) and control mice was examined on disease day 37 for expression of some genes of interest in EAE. Stimulation significantly elevated the expression of MBP (Fig. 4A), which is expressed exclusively by mature oligodendrocytes. There was a concomitant reduction in the expression of PDGFRα (Fig. 4C), which specifically marks oligodendrocyte precursor cells (OPCs). Notch1, a negative regulator of OPC differentiation, did not differ significantly between stimulated and control mice (Fig. 4B). Expression of three inflammatory cytokines that are important in MS and EAE was also measured. IFNγ and TNF were both significantly reduced by stimulation, but the effect on IL-1β did not reach significance (Figs. 4, D–F). The cytokine data showed considerably greater scatter within the stimulated group than within controls, implying random variability in treatment parameters (electrode position or duration of stimulation, for example).

Discussion

This study assumed a general model of CNS repair, in which the several raphe nuclei of the brainstem provide critical relay points in parallel restorative feedback loops. Axon terminals of raphe neurons are essentially ubiquitous in the CNS (Baumgarten and Grozdanovic, 1995), mostly releasing serotonin, a classical fast neurotransmitter that also has major neurotrophic actions (Azmitia, 2007). Conversely, serotonergic terminals in the CNS all appear to originate in cell bodies of brainstem raphe nuclei. Stimuli that cause raphe neurons to fire include some typical sensory and chemical sequelae of trauma. For example, NRM neurons respond to nociception, hypothermia, prostaglandins and hypercapnia (Fields et al., 1991; Rathner et al., 2001; Nason and Mason, 2006; Teran et al., 2014). A clinical prediction of this model is that boosting the feedback signal will enhance recovery from neurotrauma. Such proved to be the case in several of our experimental studies in rats (described in the Introduction). Additional support is here provided in a different species (mice) and a non-traumatic, neurodegenerative disease (EAE). In future, given that CNS damage is widely disseminated in progressive MS, the midbrain raphe nuclei, whose projections provide the majority of ascending serotonergic terminals, should be explored for their capacity to produce a parallel reduction of forebrain damage in EAE.

With regard to the mechanism whereby the NRM initiates this repair, part of the explanation may be found in the immune-modulatory and neuroprotective actions of serotonin (Azmitia, 2007; Berger et al., 2009). Microstimulation in the NRM has been clearly demonstrated to

release serotonin in the rat's spinal cord (Hentall et al., 2006). NRM stimulation with parameters used in this study (30 μA pulses in 8 Hz trains) has also been found to increase trophic signaling molecules cyclic AMP, pPKA and pCREB in the injured thoracic spinal cord of the rat that are blocked by the 5-HT7 receptor antagonist pimozide (Carballosa-Gonzalez et al., 2014). Furthermore, some findings with re-uptake inhibitors suggest that serotonin dampens the symptoms of EAE (White et al., 1992; Vollmar et al., 2009). Many serotonergic terminals co-release one of several neuropeptides, prominently galanin, substance P, met-enkephalin, thyrotropin-releasing hormone (Hokfelt et al., 2000; Hodges and Richerson, 2008). These are also potentially beneficial in neurodegeneration; galanin is upregulated in EAE and slows demyelination (Wraith et al., 2009; Yin et al., 2012), and thyrotropin releasing hormone and substance P also neurotrophic or protective effects (Jantas et al., 2009; Kim et al., 2015). Conceivably, serotonin and one or more of these neuropeptides have synergistic effects when simultaneously released, but spinal cord assays of these neuropeptides during and after raphe stimulation, and analysis of their specific effects, remain to be done in relevant experimental models.

Shorter-term NRM stimulation (4–7 days) had a delayed and transitory effect on EAE scores. This suggests, first, that the underlying evoked trophic changes develop over several days and, second, that causative disease factors continue to be present. Longer- term stimulation led to enduring tissue changes that outlasted the stimulation by at least several days, including increases in myelinated axons seen on day 29. The stimulation-produced rise in gene expression for MBP and decreases in PDGFRα, IFNγ and TNF seen on day 37 also outlasted the differences in overt disease between treated and control mice, which disappeared around day 28. PDGFRα marks OPCs, which thus may have differentiated into myelin-forming oligodendrocytes under the influence of the NRM stimulation. Although oligodendrocytes and their precursor cells apparently lack 5-HT receptors, astrocytes strongly express 5-HT2 and 5-HT7 receptors (Maxishima et al., 2001; Doly et al., 2005). Astrocytes in turn can bi-directionally modulate the development and functioning of oligodendrocytes (Barnett and Linington, 2013), and probably promote myelination by increasing cAMP, leading to release onto oligodendrocyte receptors of pro-myelinating signals (Ballotti et al., 1987; Xiao et al., 2010; Yin et al., 2012).

EAE is largely mediated by infiltration into the CNS of immune cells, especially lymphocytes and monocytes/macrophages, with a critical role for cytokines in amplifying the local immune response (Eng et al., 1996). EAE greatly increases expression of the three studied pro-inflammatory cytokines TNF, IFNγ and IL-1β, compared to naive mice, as observed, for example, 25 days post-induction (Madsen et al., 2016). It is important to note that the functional significance of these results is complicated, because some pro-inflammatory cytokines contribute to neuroprotection and plasticity (Schattling et al., 2014). However, in the present study, NRM stimulation enduringly reduced both the infiltration of immune cells into the spinal cord and the expression levels of these three cytokines. The infiltrating immune cells may have responded to serotonin released by the NRM in the local microenvironment, since serotonin derived from platelets regulates circulating macrophage and lymphocytes and the synthesis of cytokines such as TNF (Kubera et al., 2005; Ahern, 2011; Baganz and Blakely, 2013).

The main treatments for MS are currently provided by anti-inflammatory agents such as methylprednisolone and other immune-modulators such as interferon-β. The present findings imply that therapies directed against the neuropathic consequences of the inflammation could also prove helpful. One experimental approach may be to give a combination of mimetic drugs for serotonin and one or more neuropeptides. Another approach, stemming more directly from the present study, is electrical deep brain stimulation (DBS). DBS in the NRM is untried and appears a priori very risky for human treatment, due to its location near vital hindbrain centers, despite the apparent safety and feasibility in rodents, as revealed in the present study. This difficulty may potentially be avoided by stimulating the periaqueductal gray (PAG), an established neurosurgical target in the midbrain that has a strong, direct excitatory effect on NRM neurons (Behbehani and Fields, 1979). For MS patients, a subsidiary advantage of PAG stimulation may be reduction in debilitating pain, found in about 70% of patients with progressive MS (Foley et al., 2013). In rats, long-term PAG stimulation produced restorative effects after thoracic SCI similar to those of the NRM (Hentall and Gonzalez, 2012). A clinical trial of prolonged PAG stimulation for neuropathic pain and other degenerative symptoms of SCI is under way (Hentall et al., 2016). This same intervention might be productively explored in select groups of patients with progressive MS.

Conclusions

In a mouse model of multiple sclerosis, prolonged electrical stimulation in the brainstem (raphe magnus region) enduringly suppressed the overt disease, decreased demyelination and lowered cytokine production, thus suggesting new treatment strategies.

Acknowledgments

We would like to thank Margaret Bates and Vania Almeida of the Electron Microscopy Core Facility of The Miami Project to Cure Paralysis for their technical assistance with processing the tissue for the toluidine blue staining. We also would like to thank Mehran Taherian for assistance with mouse colony, and Aaron Perez-Castañeda for assistance with histology and image processing. This work was supported by The Danish Multiple Sclerosis Society (PMM); Fonden til Lægevidenskabens Fremme (PMM); Foundation for Research in Neurology (PMM); FISM (Italian Multiple Sclerosis Foundation) grant 2012/R/2 (RB); NIH NINDS grants NS084303-01A1 and 1RO1NS094522-01 (RB); The Miami Project To Cure Paralysis (RB, IDH), and The State of Florida (IDH).

Abbreviations

MS	multiple sclerosis
CNS	central nervous system
NRM	nucleus raphe magnus
EAE	experimental autoimmune encephalomyelitis
PCR	polymerase chain reaction
MOG_{35-55}	myelin oligodendrocyte glycoprotein 35-55 peptide fragment
ANOVA	analysis of variance

SEM	standard error of the mean
MBP	myelin basic protein
PDGFRα	platelet-derived growth factor receptor alpha
OPCs	oligodendrocyte precursor cells
IFNγ	interferon gamma
TNF	tumor necrosis factor
IL-1β	interleukin 1 beta
DBS	deep brain stimulation
PAG	periaqueductal gray

References

Ahern GP. 5-HT and the immune system. Curr Opin Pharmacol. 2011; 11:29–33. [PubMed: 21393060]

Azmitia EC. Serotonin and brain: evolution, neuroplasticity, and homeostasis. Int Rev Neurobiol. 2007; 77:31–56. [PubMed: 17178471]

Baganz NL, Blakely RD. A dialogue between the immune system and brain, spoken in the language of serotonin. ACS Chem Neurosci. 2013; 4:48–63. [PubMed: 23336044]

Ballotti R, Nielsen FC, Pringle N, Kowalski A, Richardson WD, Van Obberghen E, Gammeltoft S. Insulin-like growth factor I in cultured rat astrocytes: expression of the gene, and receptor tyrosine kinase. EMBO J. 1987; 6:3633–3639. [PubMed: 2828033]

Barnett SC, Linington C. Myelination: do astrocytes play a role? Neuroscientist. 2013; 19:442–450. [PubMed: 23131748]

Baumgarten HG, Grozdanovic Z. Psychopharmacology of central serotonergic systems. Pharmacopsychiatry. 1995; 28(Suppl):273–279.

Behbehani MM, Fields HL. Evidence that an excitatory connection between the periaqueductal gray and nucleus raphe magnus mediates stimulation produced analgesia. Brain Res. 1979; 170:85–93. [PubMed: 223721]

Berger M, Gray JA, Roth BL. The expanded biology of serotonin. Annu Rev Med. 2009; 60:355–366. [PubMed: 19630576]

Brambilla R, Ashbaugh JJ, Magliozzi R, Dellarole A, Karmally S, Szymkowski DE, Bethea JR. Inhibition of soluble tumour necrosis factor is therapeutic in experimental autoimmune encephalomyelitis and promotes axon preservation and remyelination. Brain. 2011; 134:2736–2754. [PubMed: 21908877]

Carballosa-Gonzalez MM, Vitores A, Hentall ID. Hindbrain raphe stimulation boosts cyclic adenosine monophosphate and signaling proteins in the injured spinal cord. Brain Res. 2014; 1543:165–172. [PubMed: 24246733]

Carballosa Gonzalez MM, Blaya MO, Alonso OF, Bramlett HM, Hentall ID. Midbrain raphe stimulation improves behavioral and anatomical recovery from fluid-percussion brain injury. J Neurotrauma. 2013; 30:119–130. [PubMed: 22963112]

Doly S, Fischer J, Brisorgueil MJ, Verge D, Conrath M. Pre- and postsynaptic localization of the 5-HT7 receptor in rat dorsal spinal cord: immunocytochemical evidence. J Comp Neurol. 2005; 490:256–269. [PubMed: 16082681]

Eng LF, Ghirnikar RS, Lee YL. Inflammation in EAE: role of chemokine/cytokine expression by resident and infiltrating cells. Neurochem Res. 1996; 21:511–525. [PubMed: 8734446]

Fields HL, Heinricher MM, Mason P. Neurotransmitters in nociceptive modulatory circuits. Annu Rev Neurosci. 1991; 14:219–245. [PubMed: 1674413]

Fitzner D, Simons M. Chronic progressive multiple sclerosis - pathogenesis of neurodegeneration and therapeutic strategies. Curr Neuropharmacol. 2010; 8:305–315. [PubMed: 21358979]

Foley PL, Vesterinen HM, Laird BJ, Sena ES, Colvin LA, Chandran S, MacLeod MR, Fallon MT. Prevalence and natural history of pain in adults with multiple sclerosis: systematic review and meta-analysis. Pain. 2013; 154:632–642. [PubMed: 23318126]

Friese MA, Schattling B, Fugger L. Mechanisms of neurodegeneration and axonal dysfunction in multiple sclerosis. Nat Rev Neurol. 2014; 10:225–238. [PubMed: 24638138]

Hentall ID, Zorman G, Kansky S, Fields HL. Relations among threshold, spike height, electrode distance, and conduction velocity in electrical stimulation of certain medullospinal neurons. J Neurophysiol. 1984; 51:968–977. [PubMed: 6726321]

Hentall ID, Pinzon A, Noga BR. Spatial and temporal patterns of serotonin release in the rat's lumbar spinal cord following electrical stimulation of the nucleus raphe magnus. Neuroscience. 2006; 142:893–903. [PubMed: 16890366]

Hentall ID, Burns SB. Restorative effects of stimulating medullary raphe after spinal cord injury. J Rehabil Res Dev. 2009; 46:109–122. [PubMed: 19533524]

Hentall ID, Gonzalez MM. Promotion of recovery from thoracic spinal cord contusion in rats by stimulation of medullary raphe or its midbrain input. Neurorehabil Neural Repair. 2012; 26:374–384. [PubMed: 22183979]

Hentall ID. A long-lasting wireless stimulator for small mammals. Front Neuroeng. 2013; 6:8.doi: 10.3389/fneng.2013.00008 [PubMed: 24130527]

Hentall ID, Luca CC, Widerstrom-Noga E, Vitores A, Fisher LD, Martinez-Arizala A, Jagid JR. The midbrain central gray best suppresses chronic pain with electrical stimulation at very low pulse rates in two human cases. Brain Res. 2016; 163:2119–126.

Hodges MR, Richerson GB. Contributions of 5-HT neurons to respiratory control: neuromodulatory and trophic effects. Respir Physiol Neurobiol. 2008; 164:222–232. [PubMed: 18595785]

Hokfelt T, Arvidsson U, Cullheim S, Millhorn D, Nicholas AP, Pieribone V, Seroogy K, Ulfhake B. Multiple messengers in descending serotonin neurons: localization and functional implications. J Chem Neuroanat. 2000; 18:75–86. [PubMed: 10708921]

Jantas D, Jaworska-Feil L, Lipkowski AW, Lason W. Effects of TRH and its analogues on primary cortical neuronal cell damage induced by various excitotoxic, necrotic and apoptotic agents. Neuropeptides. 2009; 43:371–385. [PubMed: 19666192]

Kim KT, Kim HJ, Cho DC, Bae JS, Park SW. Substance P stimulates proliferation of spinal neural stem cells in spinal cord injury via the mitogen-activated protein kinase signaling pathway. Spine J. 2015; 15:2055–2065. [PubMed: 25921821]

Kubera M, Maes M, Kenis G, Kim YK, Lason W. Effects of serotonin and serotonergic agonists and antagonists on the production of tumor necrosis factor alpha and interleukin-6. Psychiatry Res. 2005; 134:251–258. [PubMed: 15892984]

Madsen PM, Motti D, Karmally S, Szymkowski DE, Lambertsen KL, Bethea JR, Brambilla R. Oligodendroglial TNFR2 Mediates Membrane TNF-Dependent Repair in Experimental Autoimmune Encephalomyelitis by Promoting Oligodendrocyte Differentiation and Remyelination. J Neurosci. 2016; 36:5128–5143. [PubMed: 27147664]

Maxishima M, Shiga T, Shutoh F, Hamada S, Maeshima T, Okado N. Serotonin 2A receptor-like immunoreactivity is detected in astrocytes but not in oligodendrocytes of rat spinal cord. Brain Res. 2001; 889:270–273. [PubMed: 11166718]

Minagar A. Current and future therapies for multiple sclerosis. Scientifica (Cairo). 2013; 2013:249101.doi: 10.1155/2013/249101 [PubMed: 24278770]

Mohan H, Friese A, Albrecht S, Krumbholz M, Elliott CL, Arthur A, Menon R, Farina C, Junker A, Stadelmann C, Barnett SC, Huitinga I, Wekerle H, Hohlfeld R, Lassmann H, Kuhlmann T, Linington C, Meinl E. Transcript profiling of different types of multiple sclerosis lesions yields FGF1 as a promoter of remyelination. Acta Neuropathol Commun. 2014; 2:168.doi: 10.1186/s40478-014-0168-9 [PubMed: 25589163]

Nason MW Jr, Mason P. Medullary raphe neurons facilitate brown adipose tissue activation. J Neurosci. 2006; 26:1190–1198. [PubMed: 16436606]

Procaccini C, De Rosa V, Pucino V, Formisano L, Matarese G. Animal models of Multiple Sclerosis. Eur J Pharmacol. 2015; 759:182–191. [PubMed: 25823807]

Ransohoff RM, Hafler DA, Lucchinetti CF. Multiple sclerosis-a quiet revolution. Nat Rev Neurol. 2015; 11:134–142. [PubMed: 25686758]

Rathner JA, Owens NC, McAllen RM. Cold-activated raphe-spinal neurons in rats. J Physiol. 2001; 535:841–854. [PubMed: 11559779]

Schattling B, Eggert B, Friese MA. Acquired channelopathies as contributors to development and progression of multiple sclerosis. Exp Neurol. 2014; 262(Pt A):28–36. [PubMed: 24656770]

Teran FA, Massey CA, Richerson GB. Serotonin neurons and central respiratory chemoreception: where are we now? Prog Brain Res. 2014; 209:207–233. [PubMed: 24746050]

Vollmar P, Nessler S, Kalluri SR, Hartung HP, Hemmer B. The antidepressant venlafaxine ameliorates murine experimental autoimmune encephalomyelitis by suppression of pro-inflammatory cytokines. Int J Neuropsychopharmacol. 2009; 12:525–536. [PubMed: 18922202]

White SR, Black PC, Samathanam GK, Paros KC. Prazosin suppresses development of axonal damage in rats inoculated for experimental allergic encephalomyelitis. J Neuroimmunol. 1992; 39:211–218. [PubMed: 1353763]

Wraith DC, Pope R, Butzkueven H, Holder H, Vanderplank P, Lowrey P, Day MJ, Gundlach AL, Kilpatrick TJ, Scolding N, Wynick D. A role for galanin in human and experimental inflammatory demyelination. Proc Natl Acad Sci U S A. 2009; 106:15466–15471. [PubMed: 19717462]

Xiao J, Wong AW, Willingham MM, van den Buuse M, Kilpatrick TJ, Murray SS. Brain-derived neurotrophic factor promotes central nervous system myelination via a direct effect upon oligodendrocytes. Neurosignals. 2010; 18:186–202. [PubMed: 21242670]

Yin LL, Lin LL, Zhang L, Li L. Epimedium flavonoids ameliorate experimental autoimmune encephalomyelitis in rats by modulating neuroinflammatory and neurotrophic responses. Neuropharmacology. 2012; 63:851–862. [PubMed: 22728315]

Highlights

- We proposed that brainstem activity can reverse experimental autoimmune encephalomyelitis, a model of multiple sclerosis.
- The nucleus raphe magnus of the mouse's hindbrain was wirelessly stimulated for up to several weeks.
- The stimulation reduced overt symptoms and lastingly increased myelination.
- After stimulation, immune cell invasion and some inflammatory cytokines were lower for at least several days.
- These findings confirm the restorative role for raphe nuclei suggested by prior studies of neurotrauma

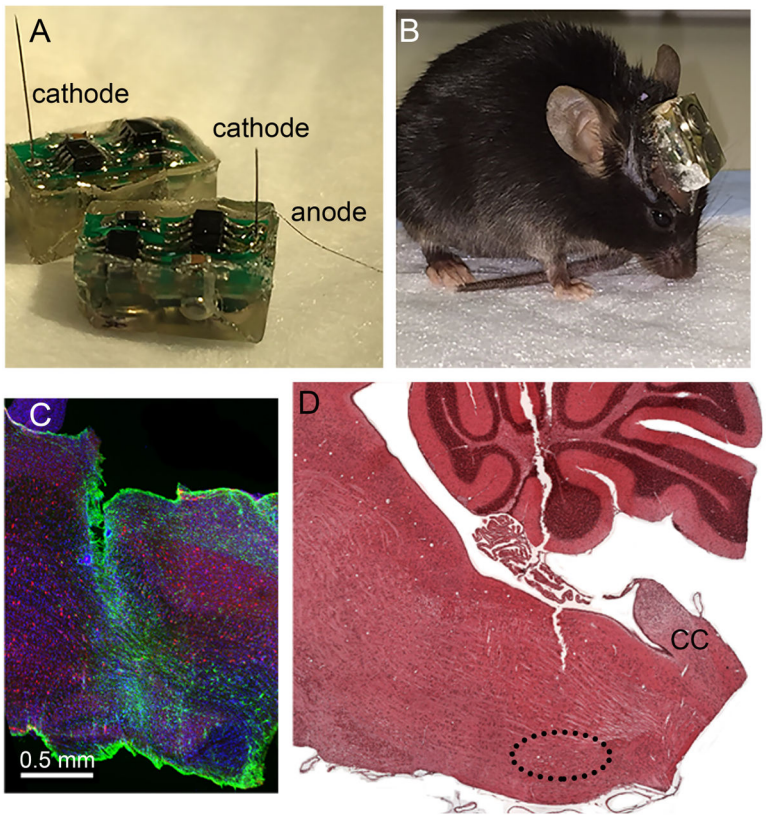

Fig. 1.

Stimulators and histology. (**A**) Encapsulated stimulators just before implantation, showing protruding electrodes (wire anode and microelectrode cathodes). (**B**) An awake mouse with an implanted working stimulator. (**C**) Immunostained sagittal section through the brainstem, including gliosis around the electrode task. Red: NeuN; green, GFAP; blue, DAPI. Scale bar = 0.5 mm. (**D**) A sagittal section through the midline of the brainstem, stained with hematoxylin-eosin, showing the approximate trajectory of the microelectrode through the cerebellum and dorsal medulla. The abbreviation CC marks the start of the spinal central canal. The dotted line outlines the NRM.

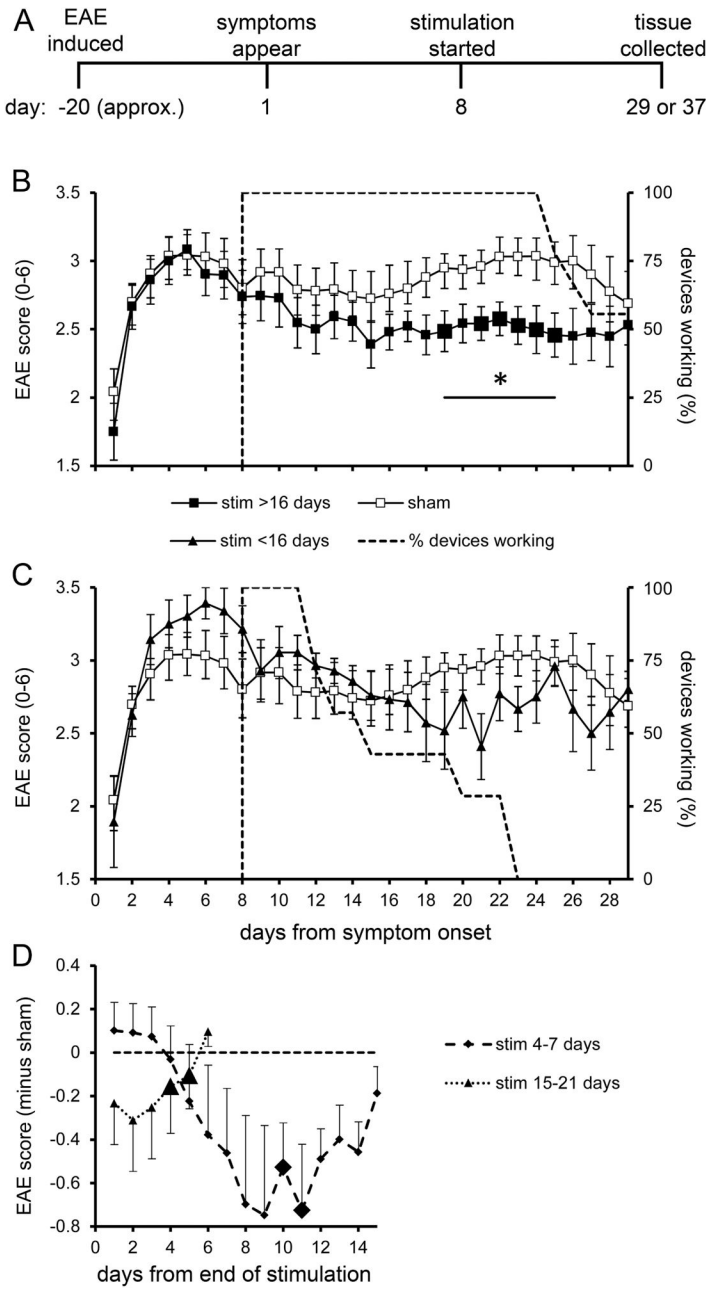

Fig. 2.

Electrical stimulation of NRM is protective in EAE. (**A**) Experimental timeline, as planned. (**B**) Time course of EAE, starting with the day of its first appearance, in the control ('sham') group and in mice receiving more than 16 days of stimulation ('stim'). Stimulation was initiated on day 8. Results are expressed as daily mean scores ± SEM; n=12 for control group and n=9 for the stimulated group. The broken line indicates the percentage of functioning stimulators on a given day. The bar marked by an asterisk shows the 7 days of peak EAE subjected to repeated measures ANOVA ($F_{1,19}$=6.71, p=0.020, partial eta-squared=0.30). Enlarged symbols indicate significant differences from the control group

found in t-tests on individual days ($p \leq 0.05$); day 19: $t_{19}=|2.24|$, p=0.040; day 21: $t_{19}=|2.28|$, p=0.037; day 22: $t_{19}=|2.23|$, p=0.041; day 23: $t_{19}=|2.67|$, p=0.017; day 24: $t_{19}=|2.80|$, p=0.013; day 25: $t_{19}=|2.55|$, p=0.022. (**C**) EAE scores for mice receiving stimulation for 4–15 days (n=7); the curve for control mice (n=12) appears also in graph B. (**D**) EAE score plotted against the numbers of days after cessation of stimulation. The daily score for an individual mouse was subtracted from the mean control score for the same post-disease day, and scores were averaged within each day counting from the end of stimulation (designated as day 1). Enlarged symbols represent significant within-subject contrasts for differences between the data point and all previous times ($p \leq 0.05$), as determined by repeated measures analysis. After stimulation for 4–7 days (n=4), days showing significant differences were day 10 ($F_{1,3}=10.4$, p=0.045, partial eta-squared=0.78) and day 11 ($F_{1,3}=10.1$, p=0.048, partial eta-squared=0.78). After stimulation for 15–21 days (n=6), days showing significant differences were day 4 ($F_{1,5}=10.6$ p=0.022, partial eta-squared=0.68) and day 5 ($F_{1,5}=7.0$, p=0.046, partial eta-squared =0.53).

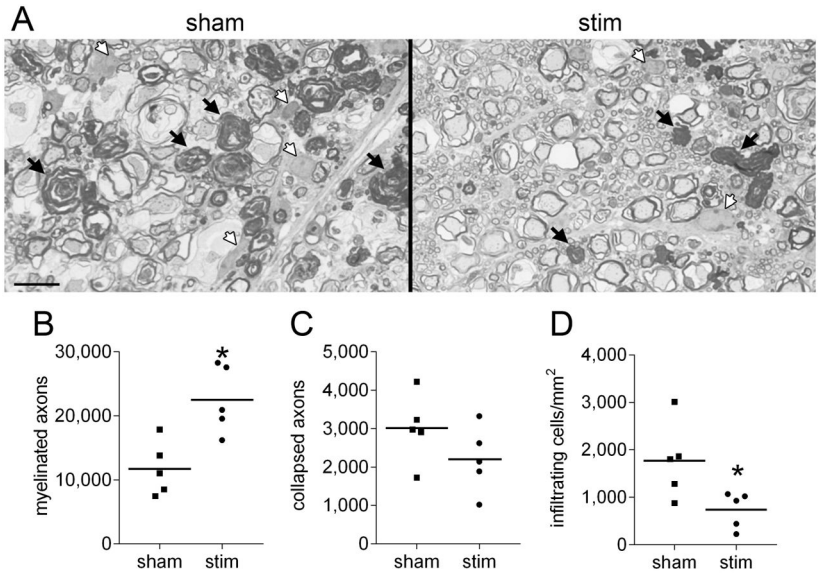

Fig. 3.

Histological analysis of spinal cord. (**A**): Toluidine blue staining of semi-thin thoracic spinal cord sections. Images of representative areas were acquired in the white matter of control ('sham') mice and stimulated ('stim') mice. Solid black arrows show collapsed axons and smaller arrows with white interiors show infiltrating cells. The scale bar in the lower left of the panel is 10 μm. Stereological quantification of myelinated axons (**B**), collapsed axons (**C**) and infiltrating cells (**D**) in the thoracic white matter of control mice (n=5) and stimulated mice (n=5). The vertical scale reflects the total counted axons within the sampled tissue (**B, C**) or infiltrating cells per area of the thin sections (**D**). Horizontal bars represent the mean. Asterisks above the column of the stimulated group indicate significant contrasts. The stimulated group received 19.4 ±1.5 (mean ±SEM) days of stimulation. Differences were significant ($p \leq 0.05$) in unpaired t-tests for myelinated axons ($t_8=3.584$, $p=0.007$, partial eta-squared=0.62) and infiltrating cells ($t_8=2.591$, $p=0.032$, partial eta-squared=0.46), but not for collapsed axons.

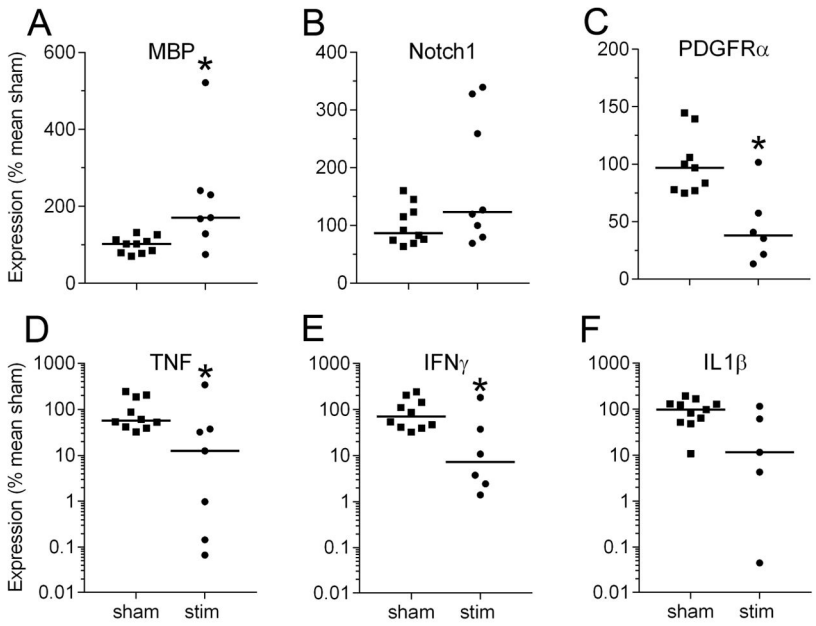

Fig. 4.

Gene expression profiling in the thoracic spinal cord after EAE. Gene expression levels were evaluated 37 days after EAE symptoms emerged in samples of control (‘sham’) mice (filled squares) and stimulated (‘stim’) mice (filled circles). Expression of the gene of interest was normalized to GAPDH expression and results in the treated group are graphed as percent of the mean of the corresponding control group. Horizontal bars indicate medians for each group. Note the cytokines (lower three graphs) are displayed on logarithmic vertical axes, which are better to show the large range of values in stimulated mice. Mean days of stimulation ranged over groups from 18.4 to 22.8. Groups sizes were MBP stimulated n=7, control n=10; Notch1 stimulated n=8, control n=10; PDGFRα stimulated n=6, control n=9; TNF stimulated n=7, control n=10; IFNγ stimulated n=6, control n=10; IL-1β stimulated n=5, control n=11. Group sizes varied due to occasional problems with the chemical assay. Significant values in the Mann-Whitney test were for MBP U=10.00, 7, 10, p=0.015; for PDGFRα U=6.00, 6, 9, p=0.012; for TNF U=11.00, 7, 10, p=0.018; for IFNγ U=9.00, 6, 10, p=0.023. Significance is indicated on graphs by an asterisk above the column of the stimulated group.

Table 1

Primers for real-time PCR gene amplification

Gene	Primer Sequence	Product Length	Optimal A_{temp}
MBP	F: 5′ cggggctctggcaaggactcacac 3′ R: 5′ tggactactgggttttcatctt 3′	101 bp	54.3°
Notch1	F: 5′ gaggtcaacgagtgcaacagtaac 3′ R: 5′ctccacccaggggcacagtcac 3′	92 bp	55.4°C
PDGFRα	F: 5′ cctggcatgatggtcgattctact 3′ R: 5′ ggtctcttctcgggctcactgttc 3′	134 bp	55.3°C
IFNγ	F: 5′ aggaactggcaaaaggatggtgac 3′ R: 5′ tgacgcttatgttgttgctgatgg 3′	118 bp	53.1°C
IL1β	F: 5′ cttcaaatctcacagcagcacatc 3′ R: 5′ ccacgggaaagacacaggtag 3′	102 bp	53.4°C
TNF	F: 5′ aggcactcccccaaaagatg 3′ R: 5′ tcaccccgaagttcagtagacaga 3′	123 bp	56.6°C
GAPDH	F: 5′ gaggccggtgctgagtatgtcgtg 3′ R: 5′ tcggcagaaggggcggagatga 3′	116 bp	59.3°C